

O.V. Kovalenko, V.Yu. Vorovsky

## Magnetic moment of $Mn^{2+}$ ions that are responsible for the ferromagnetic properties of ZnO:Mn nanocrystals

Oles Honchar Dnipro National University, Dnipro, Ukraine, [kovalenko.dnu@gmail.com](mailto:kovalenko.dnu@gmail.com)

The calculation of the magnetic moment of  $Mn^{2+}$  ions in ZnO:Mn (2 at%.) nanocrystals obtained by ultrasonic pyrolysis of aerosol which are responsible for their ferromagnetic properties is given. In order to investigate the influence of structural defects on the value of magnetic moment the samples were heat treated in air. The calculation was performed on the basis of the analysis of magnetization curves and EPR spectra. It was shown that the defective state of ZnO:Mn nanocrystals has a significant effect on the magnetic moment. The values of magnetic moment for the synthesized sample significantly exceed the values of magnetic moment compared to similar nanocrystals obtained by other methods. The assumption is made that this result is due to the presence of an additional component in the magnetization of the defective samples. In addition to the paramagnetism of  $Mn^{2+}$  ions, there may be the paramagnetism of the defective shell of ZnO:Mn nanocrystals. After the elimination of structural defects by heat treatment of samples in air and in a gas mixture with hydrogen, the magnetic moment for  $Mn^{2+}$  ions, which form the ferromagnetic properties of nanocrystals, was determined. The value of this magnetic moment is  $0.02\mu_B$ , where  $\mu_B$  is the Bohr magneton. Such ions, according to the model of bound magnetic polarons, are part of ferromagnetic clusters and take part in the formation of the ferromagnetic properties of the samples.

**Keywords:** magnetic moment, nanocrystals, ultrasonic aerosol pyrolysis, heat treatment, hydrogen.

Received 20 June 2023; Accepted 31 October 2023.

### Introduction

Dilute magnetic semiconductors (DMS) have recently been in the focus of attention due to the possibility of their practical use in the creation of spintronics devices [1]. Such materials are obtained by doping semiconductors with transition metal atoms. ZnO:Mn nanocrystals (NC), which possess ferromagnetic properties (FP) at room temperature, deserve certain attention in this respect [2,3]. The main requirement for DMS is the presence of a large value of magnetization in the saturation state  $M_s$ , which depends on the magnetic moment of the doping impurity ion. The physical nature of the FP of such materials according to the model of bound magnetic polaron (BMP) [4] is the magnetic interaction between impurity ions and intrinsic defects of the crystal lattice (CL). In this case, the intrinsic defects, such as oxygen vacancies ( $V_o$ ), act as intermediaries in the exchange interaction between impurity ions. A magnetic polaron is an electron trapped

by an oxygen vacancy  $V_o$  that interacts with the 3d electrons of impurity ions. During this interaction, the magnetic moments of the ions are oriented in the same direction. This leads to the formation of local ferromagnetic clusters, which give rise to the FP of the sample with a magnetic moment value  $\mu_f$ . In this case the electrons associated with the oxygen vacancies  $V_o$  interact with the impurity ions that are within the radius of the orbits of these electrons. The ions that are outside the orbits of these electrons are responsible for the paramagnetic properties (PP) of the sample with the value of the magnetic moment  $\mu_p$ . When samples with a higher concentration of magnetic impurity are synthesized by the same method, the concentration of  $V_o$  vacancies does not change, but there is a change in the distribution of the arrangement of impurity ions in CL. In this case, more and more ions are not united with  $V_o$  vacancies, but converge and have the opportunity to interact directly with each other. This mechanism of magnetic interaction leads to the formation of antiferromagnetic clusters with the value of

magnetic moment  $\mu_a$ , which reduce the magnetization of the samples [4]. Thus, depending on their location in the CL, the impurity ions can be in ferromagnetic, paramagnetic, and antiferromagnetic states. The problem of calculating the magnetic moments of impurity DMS ions is relevant, because this information will allow a better understanding of the mechanism of ferromagnetic ordering, as well as provide an opportunity to improve the methods of heat treatment (HT) of such materials. The purpose of this work is to evaluate the magnetic moment of Mn<sup>2+</sup> ions in ZnO:Mn NC samples obtained by ultrasonic aerosol pyrolysis (UAP), which are responsible for the formation of FP.

## I. Experiment

The average magnetic moment  $\mu$  can be determined on the basis of analysis of the samples' magnetization curves by separating the paramagnetic component. In [5] after the analysis of magnetization curves of NC ZnO:Mn (25 at.%) samples obtained by sol-gel method the average value of magnetic moment of Mn<sup>2+</sup> ions  $\mu=3.5\mu\text{B}$  was determined. A similar analysis conducted in [6] for ZnO:Mn NCs (3.9 at.%) obtained by thermal decomposition showed that the average magnetic moment of such samples has a value of  $\mu = 4.2\mu\text{B}$ . In these works the NCs were obtained at high synthesis temperatures under equilibrium conditions. We obtained ZnO:Mn (2at.%) samples under nonequilibrium conditions by the UAP method. Such samples have a defective structure in the form of a crystalline core and a defective shell with a significant number of intrinsic defects [7]. In these materials the magnetic moment of the Mn<sup>2+</sup> ions, which are responsible for the FP, has not yet been determined.

The average magnetic moment  $\mu$  per impurity atom is calculated as the result of the sum of the magnetic moments of ions in different states.

$$\mu = M/N_{Mn} = (\mu_f \cdot N_f + \mu_p \cdot N_p - \mu_a \cdot N_a)/N_{Mn}, \quad (1)$$

where  $M$  is the specific magnetization of the sample,  $\mu_f$ ,  $\mu_p$ ,  $\mu_a$  are the respective magnetic moments of the impurity atoms, and  $N_f$ ,  $N_p$ ,  $N_a$  are the concentrations of ions in the ferromagnetic, paramagnetic, antiferromagnetic states;  $N_{Mn}$  is the total concentration of impurity.

At low concentrations of impurity ions, the antiferromagnetic component can be neglected. Thus, to determine the magnetic moment  $\mu$  of ferromagnetic ions, it is necessary to separate the paramagnetic component from the magnetization curve and calculate the concentration of  $N_f$  ions in the ferromagnetic state.

In this work, the magnetic characteristics of ZnO:Mn samples with an Mn concentration of 2 at.%, which were obtained by the UAP method, are analyzed [8]. In addition to synthesized samples analysis of magnetization curves of samples after short-term HT at  $T = 550^\circ\text{C}$  and at  $T = 850^\circ\text{C}$  for 20 min, as well as after HT at  $T = 850^\circ\text{C}$  for 1 h was conducted (Fig. 1a). From the resulted magnetic characteristics of samples it is possible to draw a conclusion that magnetization curves do not have a

saturation condition. This is an indication of the presence of an additional paramagnetic component in the samples. The amount of paramagnetic phase is determined by the slope angle of the tangent lines to the experimental curves. It is known that the paramagnetic properties of samples have a linear dependence on the magnetic field  $H$ , and their magnetization is calculated as  $M = \chi H$ , where  $\chi$  is the specific susceptibility. Therefore, it is possible to separate the paramagnetic component from the experimental magnetization curves and determine the specific magnetization of the samples in the saturation state  $M_s$  (Fig. 1b). After such an analysis, the magnetic characteristics of the samples were determined (Table 1). It was shown that HT leads to a decrease in the specific magnetization  $M_s$  and the specific susceptibility  $\chi$  of the samples.

Thus the synthesized sample has a value of magnetization in the saturation state  $M_s = 0.028 \text{ emu/g}$ , and after HT at  $T = 550^\circ\text{C}$  for 20 min. this value decreases almost threefold ( $M_s = 0.01 \text{ emu/g}$ ). After HT of this sample at  $T = 850^\circ\text{C}$  for 20 min FP disappear. Nanocrystals become paramagnetic with value of specific susceptibility  $\chi = 2.53 \cdot 10^{-6} \text{ emu/gOe}$ . Heat treatment of the samples at  $T = 850^\circ\text{C}$  for 1 h. leads to the complete disappearance of the magnetic properties of the NCs.

Thus, the presence of the paramagnetic phase in the samples indicates that not all Mn<sup>2+</sup> ions take part in the formation of the FP of ZnO:Mn NC. Part of them from the total amount of  $N_{Mn}$  doping Mn impurity is paramagnetic. In accordance with the theoretical model of BMP [4], the Mn<sup>2+</sup> ions, which are located between the CL nodes at a small distance from the oxygen vacancies, are magnetically active. It is the concentration of such closely located and magnetically bound Mn<sup>2+</sup> ions ( $N_f$ ) that determines the FP of ZnO:Mn NC samples. Another part of the inter-nodal Mn<sup>2+</sup> ions ( $N_p$ ) determine the PP of the samples. There is also a certain portion of Mn<sup>2+</sup> ( $N_0$ ) ions, which are located in the ZnO ( $N_0$ ) CL nodes and do not participate in the formation of magnetic properties when there are no oxygen vacancies nearby. The proof of this is the decrease of  $M_s$  magnetization after HT of the samples in air with a simultaneous increase in the number of nodular  $N_0$  ions, which is determined by means of the EPR method. Therefore, the total amount of Mn<sup>2+</sup> ions ( $N_{Mn}$ ) in ZnO CL should be calculated according to the equation:

$$N_{Mn} = N_f + N_p + N_0. \quad (2)$$

If the number of ferromagnetic ions  $N_f$  is defined as  $N_f = M_s/\mu$ , and the number of paramagnetic  $N_p$  ions Mn<sup>2+</sup> is obtained from the well-known Curie equation:

$$\chi = N_p(\mu)^2/3kT, \quad (3)$$

where  $\chi$  is specific magnetic susceptibility of paramagnetic Mn<sup>2+</sup> ions;  $k$  is Boltzmann constant,  $T$  is sample temperature, then on the base of (2) we have a quadratic equation regarding mean value of magnetic moment :

$$\mu - \mu \frac{M_s}{(N_{Mn} - N_0)} - \frac{\chi 3kT}{(N_{Mn} - N_0)} = 0, \quad (4)$$

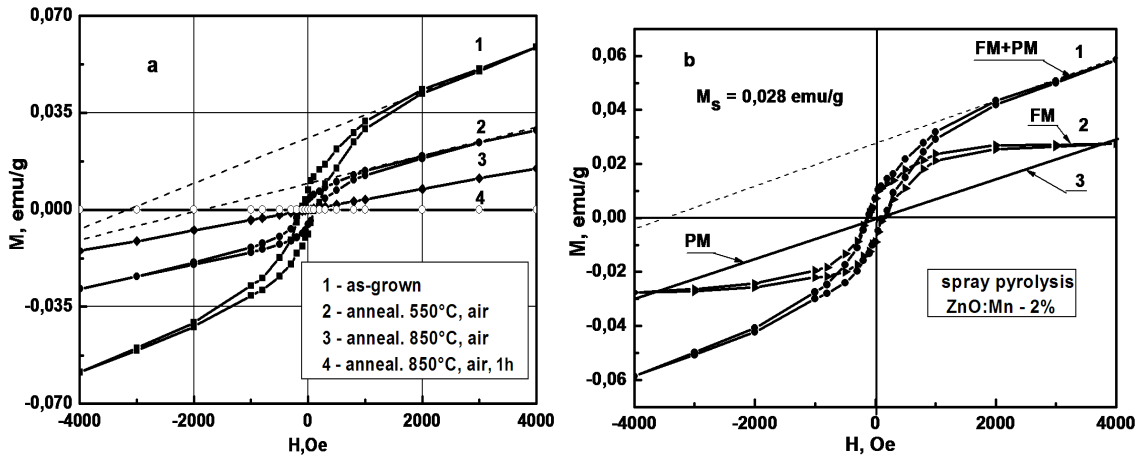


**Fig.1.** Magnetization curves of NC ZnO:Mn (2at.%) (a): 1 - synthesized sample, 2 - sample after HT in air at  $T=550^\circ\text{C}$ , 20 min, 3 - sample after HT in air at  $T=850^\circ\text{C}$ , 20 min, 4 - sample after HT in air at  $T=850^\circ\text{C}$ , 1 hour. Decomposition of the experimental magnetization curve of the sample (1) into ferromagnetic (FM) and paramagnetic (PM) components (b) [8].

**Table 1.**

Components of magnetization of ZnO:Mn NC samples (2 at.%)

| № | Type of samples                                      | Ferromagnetic component | Paramagnetic component |
|---|--|-------------------------|------------------------|
|   |  | $M_s$ , emu/g           | $\chi$ , emu/g·Oe      |
| 1 | Synthesized sample ZnO:Mn (2at.%)                    | 0,028                   | $7,35 \times 10^{-6}$  |
| 2 | Sample after HT at $T = 550^\circ\text{C}$ , 20 min. | 0,01                    | $5,50 \times 10^{-6}$  |
| 3 | Sample after HT at $T = 850^\circ\text{C}$ , 20 min. | -                       | $2,53 \times 10^{-6}$  |
| 4 | Sample after HT at $T = 850^\circ\text{C}$ , 1 h.    | -                       | -                      |

The concentration of nodal  $N_0$   $\text{Mn}^{2+}$  ions was determined by EPR by analyzing the hyperfine structure (HFS) lines of the EPR spectra and calculating their integral areas. The EPR spectra of all samples (Fig. 2a) were normalized by mass of the substance. The concentration of nodal  $\text{Mn}^{2+}$  ions was calculated according to the formula:

$$N_0 = N_e S / S_e, \quad (5)$$

where  $N_e$  is the concentration of  $\text{Mn}^{2+}$  ions in the reference sample  $\text{CuSO}_4 \cdot 6\text{H}_2\text{O}$  ( $N_e = 2.4 \cdot 10^{21}$  1/g);  $S$  is the total integral area of the HFS lines of the EPR spectrum of the sample;  $S_e$  is the integral area of the line EPR spectrum of the reference sample in relative units.

Peculiarity of ESR spectra of samples obtained by the UAP method (Fig. 1a, line 1) is their asymmetric form. It is a consequence of the presence of ferromagnetic clusters and structural defects in CL in the samples, which lead to local structural disorder around Mn ions, such as dislocations.

The increased intensity of HFS lines during HT (Fig.2a) indicates that  $\text{Mn}^{2+}$  ions take up their positions in the CL nodes isovalently replacing  $\text{Zn}^{2+}$  ions and becoming nodular ions. After HT of ZnO:Mn sample in air at  $T = 850^\circ\text{C}$  almost all structural defects disappear, asymmetry of the spectrum also almost vanishes. The EPR spectrum of the sample contains only HFS lines and a broad absorption line caused by dipole interaction of  $\text{Mn}^{2+}$  ions. The high intensity of the HFS lines indicates a significant amount of  $\text{Mn}^{2+}$  ions, which took part in the

doping of ZnO NCs. The asymmetric structure of the EPR spectra complicates the analysis of the HFS lines. Therefore, we carried out a procedure to separate the HFS lines from the EPR spectra by separating the averaging line (2) from the experimental line (1) - dotted line in Fig.2b. Results of calculations of concentration  $N_0$  of knotty  $\text{Mn}^{2+}$  ions for all samples and their percentage ratio to total concentration of  $N_{\text{Mn}}$  ions are given in Table 2. It should be noted that the obtained value of the amount of nodular  $N_0$   $\text{Mn}^{2+}$  ions in the synthesized sample  $N_0 = 2.2 \cdot 10^{17}$  1/g practically coincides with the results obtained in [9] for the sample ZnO: Mn (2 at.%), which found that  $N_0 = 3.1 \cdot 10^{17}$  1/g.

The obtained results indicate a low level of alloying of ZnO NC with Mn impurity during synthesis by UAP method. Compared with the total concentration of  $\text{Mn}^{2+}$  ions (2 at.%, the value of  $N_{\text{Mn}} = 1.49 \cdot 10^{20}$  1/g) the concentration of nodular  $N_0$   $\text{Mn}^{2+}$  ions in the synthesized samples is approximately 0.15%. This result is to be expected because the doping process during synthesis takes place in non-equilibrium conditions for a short period of time (7–10 s). During the HT of the synthesised sample at  $T = 550^\circ\text{C}$  the amount of  $\text{Mn}^{2+}$  nodular ions increases to 0.24%, but even after HT at  $T = 850^\circ\text{C}$  for 1 hour it does not exceed 5.6%. The results of calculations of  $\mu$  value according to equation (4) are also given in Table 2. The obtained  $\mu$  values were used to determine the quantitative composition of  $\text{Mn}^{2+}$  ions in ZnO:Mn (2 at.%) CL. The concentration of  $N_{\text{P}}$  paramagnetic  $\text{Mn}^{2+}$  ions was determined from equation (2). Total concentrations of  $\text{Mn}^{2+}$  ions ( $N_0$ ,  $N_{\text{F}}$ ,  $N_{\text{P}}$ ) in the samples are given in Table 2.

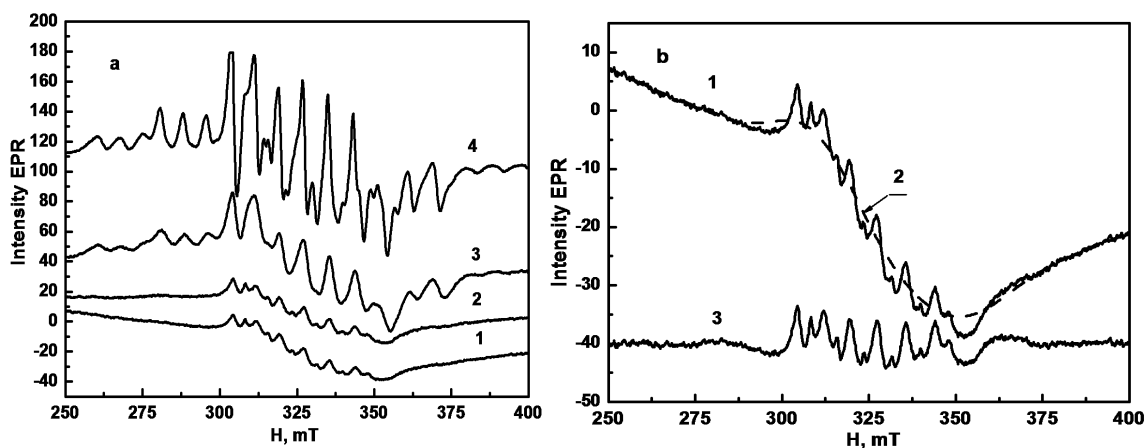


**Fig.2.** EPR spectra of ZnO:Mn (2 at.%) NC samples (a): 1 - synthesized sample; 2 - sample after HT in air at  $T=550\text{ }^{\circ}\text{C}$ , 20 min.; 3 - sample after HT in air at  $T = 850\text{ }^{\circ}\text{C}$ , 20 min.; 4 - sample after HT in air at  $T = 850\text{ }^{\circ}\text{C}$ , 1 h. The EPR spectrum of the synthesized sample (b): 1 - experimental line; 2 - averaged line (dotted line); 3 - separated HFS line of Mn<sup>2+</sup> ions.

**Table 2.**

| Concentration of Mn <sup>2+</sup> ions ( $N_0$ , $N_f$ , $N_p$ ) and magnetic moment $\mu$ |   |                              |                  |                              |                              |                       |
|--|---|------------------------------|------------------|------------------------------|------------------------------|-----------------------|
| $N_0$  | Type of samples                                 | $N_0 \cdot 10^{17}$ ,<br>1/g | $N_0/N_{Mn}$ , % | $N_f \cdot 10^{17}$ ,<br>1/g | $N_p \cdot 10^{20}$ ,<br>1/g | $\mu$ , $\mu\text{B}$ |
| 1  | Synthesized ZnO:Mn (2at.%)                      | 2,2                          | 0,15             | 3,5                          | 1,477                        | 8,5                   |
| 2  | After HT at $T = 550^{\circ}\text{C}$ , 20 min. | 3,6                          | 0,24             | 1,6                          | 1,475                        | 6,6                   |
| 3  | After HT at $T = 850^{\circ}\text{C}$ , 20 min. | 35,0                         | 2,3              | -                            | 1,445                        | 5,1                   |
| 4  | After HT at $T = 850^{\circ}\text{C}$ , 1 h     | 84,0                         | 5,6              | -                            | -                            | -                     |

The calculations show that the CL defects have a significant influence on the magnetic moment  $\mu$ . The synthesized sample has a magnetic moment  $\mu = 8.5\ \mu\text{B}$ . This value decreases during annealing of the sample at  $T = 550^{\circ}\text{C}$ , 20 min. to a value of  $\mu = 6.6\ \mu\text{B}$ , and at  $T = 850^{\circ}\text{C}$ , 20 min. - to a value of  $\mu = 5.1\ \mu\text{B}$ . It follows from Table 1. that the value of specific susceptibility  $\chi$ , which is included in equation (3), will also decrease after HT. At the same time the values of  $\mu$  ( as well as the values of  $\chi$  ) remain quite large compared to the data obtained in [5,6]. It is possible that such values of specific susceptibility  $\chi$  are due to the presence of an additional source of paramagnetism, which contributes to the paramagnetic component of sample magnetization. This source may be paramagnetism of the deformed surface layer of ZnO:Mn NC. It is known that not only atoms have paramagnetic properties, but also structural defects of CL with an odd number of electrons. In [10] increase of magnetic susceptibility  $\chi$  after deformation of Zn monocrystals was established. It is shown that this phenomenon is caused by the appearance of a surface deformation layer with dislocation-type defects in monocrystals. It is possible that the surface layer in such monocrystals is actually connected with zinc oxide. Chemical removal of this layer leads to disappearance of magnetic effects. It is known that ZnO:Mn NCs (2 at.%), whose magnetic properties are investigated in this work, have a defective structure in the form of a defect-free core and a defective shell [7]. Therefore we can assume that such a near-surface NC layer may have structural defects - dislocations, acquire paramagnetic properties, and contribute to the paramagnetic component of the sample magnetization.

To exclude the influence of defects on the calculation of magnetic moment  $\mu$  we additionally analyzed magnetization curves and EPR spectra of NC samples ZnO:Mn (2at.%) [11] obtained after HT in air at  $T = 850^{\circ}\text{C}$ , 20 min and after HT in hydrogen at  $T = 550^{\circ}\text{C}$ . After HT in air the majority of structural defects in CL disappear and the sample acquires paramagnetic properties with the value of specific susceptibility  $\chi = 2.53 \cdot 10^{-6}\ \text{emu/gOe}$  (Fig.3a). After the following HT in hydrogen, the sample is converted to a ferromagnetic state at which the magnetization curve has a clear saturation state. The absence of structural defects (dislocations) in the sample after annealing in hydrogen is proved by the symmetry of the absorption line of its EPR spectrum (Fig. 3b, line 2), compared to the asymmetric EPR spectrum of the synthesised sample (Fig. 3b, line 1). The EPR spectrum line of the sample after annealing in hydrogen is structureless and has a high intensity. A significant increase in the amplitude of the EPR line is due to the action of hydrogen, which forms a large number of intrinsic defects, oxygen vacancies, hydroxyl groups, and  $(V_o + H)^{2+}$  complexes in NCs [12]. All these defects have electrons with uncompensated spins and therefore make an additional contribution to the EPR absorption line. At the same time, the reduction of FP occurs as a consequence of the interaction of oxygen vacancies  $V_o$  and inter-nodal Mn<sup>2+</sup> ions on the NC surface. These ions remained after annealing of the sample in air at  $T=850^{\circ}\text{C}$  and caused its PP.

Thus, the presence of  $V_o$  vacancies and inter-nodal Mn<sup>2+</sup> ions in accordance with the BMP model creates conditions for the occurrence of FP. An important result is that the magnetization curve after HT in hydrogen has a

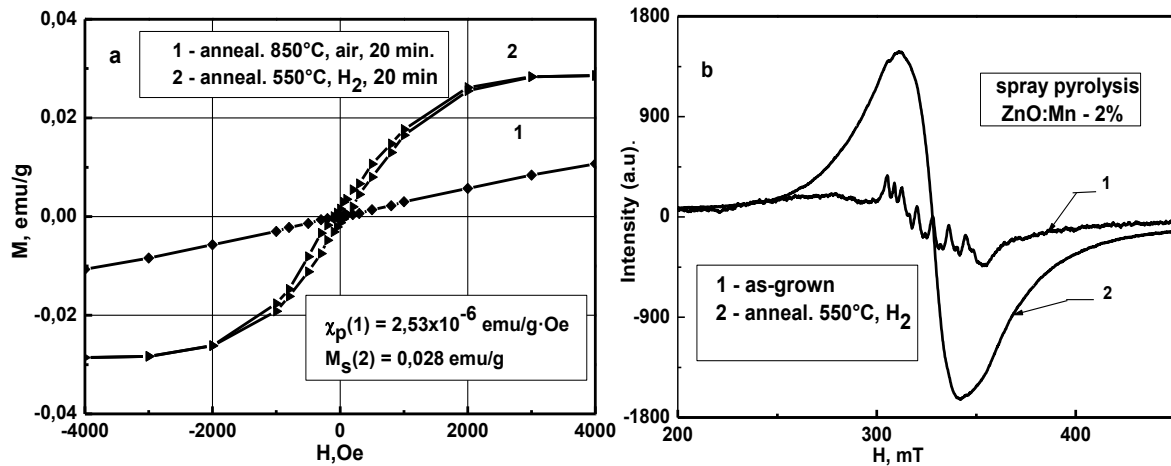


**Fig.3.** Magnetization curves (a): 1 – sample after HT in air at  $T = 850^{\circ}\text{C}$  for 20 min, 2 – sample after subsequent HT in hydrogen at  $T = 550^{\circ}\text{C}$  for 20 min; EPR spectra (b): 1 – synthesized sample, 2 – sample after subsequent HT in hydrogen at  $T = 550^{\circ}\text{C}$  for 20 min. [11].

saturation state. This indicates that the number of oxygen vacancies  $V_0$  exceeds the number of impurity  $\text{Mn}^{2+}$  ions:  $N(V_0) > N(\text{Mn}^{2+})$ . Due to the large number of  $V_0$  during the hydrogen HT, practically all inter-nodular, paramagnetic  $\text{Mn}^{2+}$  ions take part in the formation of ferromagnetic clusters. Thus, the paramagnetic ions become ferromagnetic. It is

important to note that the amount of inter-nodal  $\text{Mn}^{2+}$  ions does not change after annealing in hydrogen at low temperature ( $T = 550^{\circ}\text{C}$ ), so  $N_f = N_p = 1.445 \cdot 10^{20} \text{1/g}$ . This amount is approximately equal to the total amount of impurity ions ( $N_{\text{Mn}} = 1.49 \cdot 10^{20} \text{1/g}$ ) in the synthesized samples. In turn, a correct calculation of the magnetic moment of ferromagnetic  $\text{Mn}^{2+}$  ions can now be made from the ratio  $\mu_f = M_s/N_f = 0.02 \mu_B$ .

## Conclusions

The calculation of average magnetic moment  $\mu$  of  $\text{Mn}^{2+}$  ion in  $\text{ZnO:Mn}$  NC (2 at.%) at different defective states of CL which were achieved by HT of samples was made. On the basis of experimental studies it is supposed that  $\text{Mn}^{2+}$  ions replacing  $\text{Zn}^{2+}$  ions in  $\text{ZnO}$  CL nodes do not take part in the formation of FP of samples. The calculation of  $\text{Mn}^{2+}$  ( $N_0$ ) nodules amount has shown the low level of  $\text{ZnO}$  NC doping with Mn impurity during

UAP synthesis. It is proved that the defective near-surface layer of  $\text{ZnO:Mn}$  NC has PP and gives an additional contribution to the paramagnetic component of sample magnetization. Air curing of samples leads to decrease and disappearance of FP. In order to eliminate the influence of defects on the calculation of  $\mu$  a procedure of successive short-term HT of the samples in air and then in hydrogen was proposed. After this HT the sample becomes ferromagnetic again and the amount of ferromagnetic  $\text{Mn}^{2+}$  ions becomes equal to the amount of paramagnetic  $\text{Mn}^{2+}$  ions. Based on this, the value of magnetic moment  $\mu_f$  of ferromagnetic  $\text{Mn}^{2+}$  ions, which are part of ferromagnetic clusters according to the BMP model, is calculated. This value is equal to:  $\mu_f = 0.02 \mu_B$ . The results allow us to understand the mechanism of ferromagnetic ordering and give an opportunity to improve the methods of HT to produce nanocrystals with predictable physical properties..

**Kovalenko O.V.** - Doctor of Physical and Mathematical Sciences, Professor, Head of the Department of Applied Radiophysics, Electronics and Nanomaterials.

**Vorovsky V. Yu.** - Head of the Laboratory of the Department of Applied Radiophysics, Electronics and Nanomaterials.

- [1] T. Dietl, H. Ohno, *Dilute ferromagnetic semiconductors: Physics and spintronic structures*, Rev. Mod. Phys., 86, 187 (2014); <https://doi.org/10.1103/RevModPhys.86.187>.
- [2] K. Sebayang, D. Aryanto, S. Simbolon et al., *Effect of sintering temperature on the microstructure, electrical and magnetic properties of Zn<sub>0.98</sub>Mn<sub>0.02</sub>O material*, IOP Conf. Series: Materials Science and Engineering, 309, 012119 (2018); <https://doi.org/10.1088/1757-899X/309/1/012119>.
- [3] M. Mustaqima, C. Liu, *ZnO-based nanostructures for diluted magnetic semiconductor*, Turkish Journal of Physics, 38 (3), 429 (2014); <https://doi.org/10.3906/fiz-1405-17>.
- [4] J.M.D. Coey, M. Venkatesan, C.B. Fitzgerald, *Donor impurity band exchange in dilute ferromagnetic oxides*, J. Nature Mater., 4 173 (2005); <https://doi.org/10.1038/nmat1310>.

- [5] A.M. Abdel Hakeem, *Room-temperature ferromagnetism in  $Zn_{1-x}Mn_xO$* , J. Magn. Magn. Mater., 322 (6), 709 (2010); <https://doi.org/10.1016/j.jmmm.2009.10.046>.
- [6] M. El-Hilo, A.A. Dakhel, *Structural and magnetic properties of Mn-doped ZnO powders*, J. Magn. Magn. Mater., 323, 2202 (2011); <https://doi.org/10.1016/j.jmmm.2011.03.031>.
- [7] O. V. Kovalenko, M. F. Bulaniy, V. Y. Vorovskiy, O.V. Khmelenko, *Photoluminescence and EPR spectrum of ZnO:Mn nanocrystals*, Journal of Physics and Electronics 26 (1), 69 (2018); <https://doi.org/10.15421/331811>.
- [8] O.V. Kovalenko, V.Yu. Vorovsky, O.V. Khmelenko, *The effect of heat treatment on the magnetic properties of ZnO:Mn nanocrystals obtained by ultrasonic aerosol pyrolysis*, Functional Materials 27(4), 687 (2020); <https://doi.org/10.15407/fm27.04.687>.
- [9] A. Abdel-Galil, M.R. Balboul, A. Sharaf, *Synthesis and characterization of Mn-doped ZnO diluted magnetic semiconductors*, Phys B, 477, 20 (2015); <http://dx.doi.org/10.1016/j.physb.2015.08.001>.
- [10] O.V. Brodovij, et al., *Magnetic Deformation Effect*, Usp. Fiz. Met., 2, 131 (2001); <https://doi.org/10.15407/ufm.02.02.131>.
- [11] O.V. Kovalenko, V.Yu. Vorovsky, O.V. Khmelenko, O.I. Kushnerov, *Effect of short-term heat treatment in the hydrogen on magnetic properties of ZnO:Mn nanocrystals*, Journal Physics and Chemistry of Solid State, 23 (3), 569 (2022); <https://doi.org/10.15330/pcss.23.3.569-574>.
- [12] E. V. Lavrov, F. Herklotz, and J. Weber, *Identification of two hydrogen donors in ZnO*, Phys. Rev. B 79, 165210 (2009); <https://doi.org/10.1103/PhysRevB.79.165210>.

О.В. Коваленко, В.Ю. Воровський

## Магнітний момент іонів $Mn^{2+}$ , які обумовлюють ферромагнітні властивості нанокристалів ZnO:Mn

Дніпровський національний університет імені Олеся Гончара, м.Дніпро, [kovalenko.dnu@gmail.com](mailto:kovalenko.dnu@gmail.com);

Приведено розрахунок магнітного моменту іонів  $Mn^{2+}$  в нанокристалах ZnO:Mn (2 ат%) отриманих методом ультразвукового піролізу аерозолу, які відповідають за ферромагнітні властивості. З метою дослідження впливу структурних дефектів на значення магнітного моменту проведено термічну обробку зразків на повітрі. Розрахунок виконувався на основі аналізу кривих намагніченості та спектрів ЕПР. Показано, що дефектний стан нанокристалів ZnO:Mn має значний вплив на магнітний момент. Значення магнітного моменту для синтезованого зразку значно перевищують значення магнітного моменту в порівнянні з подібними нанокристалом отриманими іншими методами. Зроблено припущення, що такий результат обумовлений наявністю у намагніченості дефектних зразків додаткової складової. Окрім парамагнетизму іонів  $Mn^{2+}$  може існувати парамагнетизм дефектної оболонки нанокристалів ZnO:Mn. Після усунення структурних дефектів шляхом термічної обробки зразків на повітрі та у газовій суміші з воднем визначено магнітний момент для іонів  $Mn^{2+}$ , які формують ферромагнітні властивості нанокристалів. Величина цього магнітного моменту дорівнює  $0,02\mu_B$ , де  $\mu_B$  – магнітон Бору. Такі іони, згідно моделі зв'язаних магнітних поляронів, входять до складу ферромагнітних кластерів та приймають участь у формуванні ферромагнітних властивостей зразків.

**Ключові слова:** магнітний момент, ультразвуковий піроліз аерозолу, термічна обробка, водень.